PHYSICAL REVIEW B VOLUME 25, NUMBER 4 15 FEBRUARY 1982

Single-particle and collective excitations in ferromagnetic iron from electron-energy-loss spectroscopy

E. Colavita, M. De Crescenzi, L. Papagno, R. Scarmozzino, L. S. Caputi, and R. Rosei
Dipartimento di Fisica, Universitá della Calabria, Arcavacata di Rende, Cosenza, Italy

E. Tosatti
Gruppo Nazionale di Struttura della Materia—Consiglio Nazionale delle Ricerche, Istituto di Fisica Teorica, Universitá di Trieste and Scuola Internazionale Superiore di Studi Avanzati and International Center for Theoretical Physics, Trieste, Italy
(Received 23 June 1981)

Electron-energy-loss spectra have been taken on clean and oxygen-covered polycrystalline iron samples. The results are discussed in terms of their dependence on the surface oxidation and on the primary electron energies. Bulk and surface collective excitations are identified. Single-particle interband transitions are found in excellent agreement with previous optical results. A new strong transition around 10 eV, not present in optical experiments, is identified as a dipole-forbidden but quadrupole-allowed process. Interband transitions are interpreted in terms of the band structure calculated by Callaway and Wang, which is thus checked up to much higher energies than previously possible. The agreement of the band structure with our experimental results can be improved at high energies by shifting the calculated conduction bands downward in energy by about 1 eV.

I. INTRODUCTION

The electronic structure of iron is still relatively poorly known, despite its enormous technological importance. Experimental difficulties (mostly related to the high chemical reactivity towards oxidizing agents) and theoretical difficulties (related to the formulation of a proper theory of itinerant ferromagnetism[1]) have delayed the understanding of the electronic properties of Fe with respect to those of other transition metals.

Experimental optical studies have recently been reported in the 0.5—4.0-eV photon energy range[2] as well as in the vacumm ultraviolet (4—27 eV).[3] The interpretation of these optical spectra in terms of band-structure calculations has however been confined to the low photon energy.[2] Several photoemission studies have also appeared in the last few years.[4,5] Of particular relevance are studies of angle-resolved photoemission,[5] which have determined exchange-split filled energy-band dispersions along selected symmetry lines. These results compare very well with band calculations of Callaway and Wang[6] performed within the framework of a Stoner-Wohlfarth-Slater with a von Barth—Hedin-type exchange correlation potential.

Energy loss spectroscopy (ELS) has been shown to be a valuable technique for investigating the electronic structure of solids,[7,8] and we have undertaken ELS measurements of ferromagnetic iron with the aim of elucidating further its electronic properties. We have measured spectra on atomically clean polycrystalline surfaces and on oxygen covered Fe surfaces at several different primary electron energies. We have also implemented a simple theoretical model which has allowed us to identify the position of single-particle interband excitations in the spectra, as minima in the function $(-d^2/dE^2)\,[EN(E)]$. The energy location of interband transitions has allowed us to test existing theoretical band calculations up to about 25 eV. We have found that similarly to other transition metals[9] and noble metals,[10] a good correlation exists between ELS structures and structures in the loss function as calculated from optical spectra via Kramers-Kronig analysis. This correlation, however, breaks down for a transition which appears in the clean Fe ELS spectrum at 10.4 eV but it is missing in optical spectra.[11] We interpret this feature as a quadrupole-allowed transition on the basis of a general discussion of quadrupole transitions in a bcc crystal.

Multipole transitions have been seen previously in ELS core-level spectra[12] but this is, to our knowledge, the first time that it has been detected in the interband region of the spectrum. We per-

formed also a study of longitudinal excitations which are located at peaks of $(-d^2/dE^2)[EN(E)]$.[11] A collective excitation found at 22.4 eV has been identified as a bulk plasmon. Only a single weak feature at 12 eV was found to behave as a surface excitation (disappearing on increasing the primary electron energy or oxygen coverage) and it was interpreted as a surface plasmon.

We studied oxygen-coverage dependence of ELS spectra in order to separate surface features from bulk features and we find only weak surface effects.

II. EXPERIMENTAL TECHNIQUE AND RESULTS

The experiments were performed using a Varian single-pass cylindrical mirror analizer (CMA) (resolution $\Delta E/E=0.6\%$) with a coaxial electron gun. Normal incidence of the electron beam was used in both ELS and Auger measurements. The energy-loss spectra were obtained in the second derivative mode for several primary electron energies E_p. A small voltage ($V_{p-p}\gtrsim 0.2$ V) was supplied to the outer cylinder of the CMA and was used as a reference for a lock-in amplifier. The full width at half maximum of the elastic peak was about 0.6 eV for a primary energy $E_p=120$ eV.

A high-purity polycrystalline rod of Fe was cut to size ($3\times4\times4$ mm^3) and mechanically polished with 12-μm alumina abrasive. The damaged surface layer was removed by chemical etching. Before each set of measurements a clean Fe surface was prepared by several cycles of Kr^+-ion bombardment (6 kV, 10 μA/cm^2, 5 min) using an Atomika ion gun equipped with a differential pumping system. The partial Kr pressure was always below 10^{-9} Torr during the cleaning process. The base pressure of the chamber ($p\simeq10^{-10}$ Torr) was reached within 5 min after each ion bombardment cycle. No impurities were observed on the surface within our Auger detection limit ($\lesssim 1\%$). Surface cleanliness was monitored again after each ELS run. The ELS spectra of clean Fe surfaces taken at 50, 90, 120, and 200 eV are shown in Fig. 1. Several features are visible and have been labeled as peaks *A*, *B*, *C*, *D*, *E*, *F*, *G*, and *H*. The most prominent of these features (*A*, *B*, *F*, *G*, and *H*) do not exibit a marked dependence on the primary electron energy E_p.

The behavior of the weaker structures (*C*, *D*, and *E*) is less clear. A series of measurements as a function of oxygen coverages was taken to clarify their nature. These results are shown in Fig. 2. Peaks *A*, *B*, *F*, *G*, and *H* are remarkably independent of oxygen coverages up to about $\frac{1}{10}$ of a monolayer. On the contrary, the oxygen does affect the weak features *C*, *D*, and *E*. The shoulder at 12 eV completely disappears even at our lowest oxygen coverage, while the behavior of peaks *C* and *D* is more complex. At about 0.1 monolayers of oxygen, these peaks are much stronger but still discernible as separate features. At higher coverages they merge in a single strong feature centered at about 8 eV.

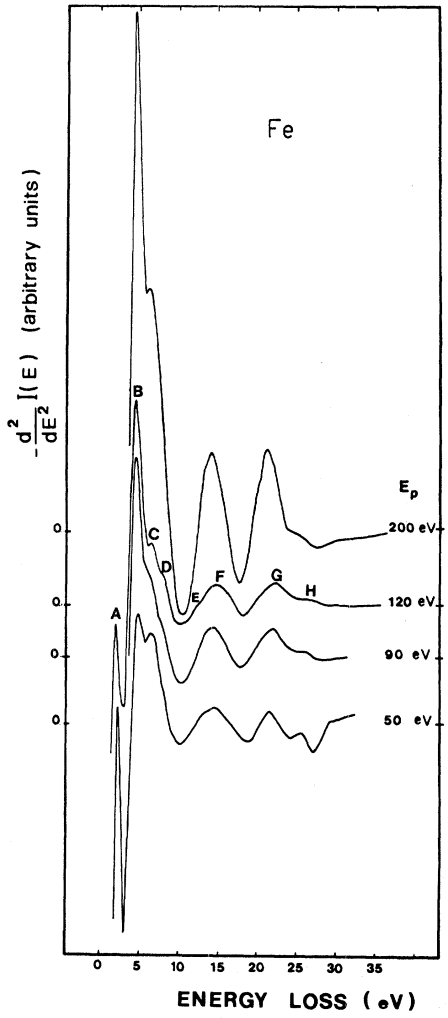

FIG. 1. Electron-energy-loss spectra measured with the primary electron energies $E_p=200$, 120, 90, and 50 eV. For clarity the first loss at 1.8 eV is shown only for $E_p=120$ and 50 eV.

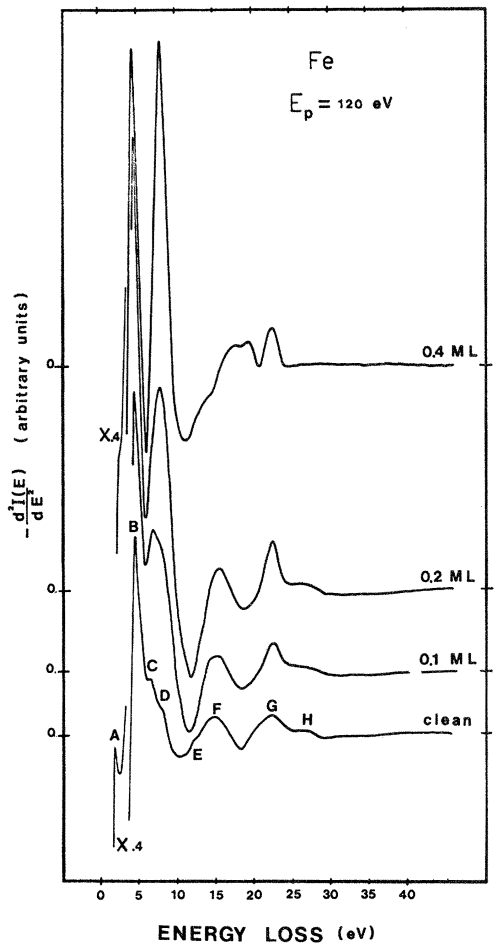

FIG. 2. Electron-energy-loss spectra taken at $E_p = 120$ eV at different oxygen coverages. The first loss at 1.8 eV, well resolved for the clean surface, smears by increasing the oxygen contamination.

III. PHENOMENOLOGICAL

Based on classical,[7] semiclassical,[13] or quantum-mechanical considerations,[14] the energy-loss probability for an electron penetrating a depth d below the surface of a medium of dielectric function $\tilde{\epsilon}(E)$ (neglecting spatial dispersion) can be taken of the form

$$N(E)=dB(E_p,E)\,\mathrm{Im}\left[-\frac{1}{\tilde{\epsilon}}\right]+S(E_p,E)\,\mathrm{Im}\left[-\frac{1}{\tilde{\epsilon}+1}\right]. \tag{3.1}$$

The first term is the bulk contribution while the second term gives the surface contribution.

In reflection ELS, the energy-loss rate can be assumed to be just twice the form above, if the reflection is supposed to occur through elastic scattering. However, the depth d must now be specified as a function of E_p. One sensible procedure would be to set $d=l(E_p)$, where l is the average penetration depth, well known for most materials.[15] The indicated dependence of the coefficients B and S is generally not known, except for very large primary electron energies E_p. In this case one can get—from direct integration over q of Ritchie's formulas[13]—the limiting behavior $B\simeq E_p^{-1}\ln(E_0E_p/E^2)$ and $S\simeq E_0^2/E_pE$, where E_0 is a fixed energy parameter of the order of $\hbar^2/2ma^2$ (a is the lattice parameter). These asymptotic formulas can be considered valid for E_p above 100 eV or so. In this regime, therefore, it is expected that the bulk transitions become more important as E_p increases, both because $l(E_p)$ increases and because B decreases slower than S. For E_p much lower that 100 eV, $l(E_p)$ increases again, but B and S become totally unkown. Preliminary indications in (Ref. 16) are that, despite the increase of $l(E_p)$, the bulk term keeps decreasing in importance as E_p lowers. This allows the conclusion generally followed,[12,17] that one can, in principle, distinguish surface contributions in ELS by varying E_p, and looking for structures that are enhanced at lower E_p.

The ELS spectra measure the quantity

$$M(E)=-\frac{d^2}{dE^2}[EN(E)]\,. \tag{3.2}$$

clearly a complicated function of E. Since, however, the prefactor E in (3.2) generates a weak E dependence in $M(E)$, and furthermore there is no reason to suspect a strong dependence of B and S from E, we can put (3.1) into (3.2) and describe the result approximately as

$$M(E)=-2lBE\frac{d^2}{dE^2}\left[-\mathrm{Im}\left[\frac{1}{\tilde{\epsilon}}\right]\right]-2SE\frac{d^2}{dE^2}\left[-\mathrm{Im}\left[\frac{1}{\tilde{\epsilon}+1}\right]\right]+\ldots, \tag{3.3}$$

where the ellipsis represent slowly varying terms.

Therefore, if $\tilde{\epsilon}(E)$ (Ref. 18) were known from independent sources, the behavior of $M(E)$ could be calculated. We have generated a rather accurate optical $\tilde{\epsilon}(E)$ via Kramers-Kronig analysis, using the low-energy reflectivity data of Ref. 2 and the high-energy data reported by Moravec *et al.*[3] From this we have calculated the surface and bulk loss functions $-\mathrm{Im}(\tilde{\epsilon}+1)^{-1}$ and $-\mathrm{Im}(\tilde{\epsilon})^{-1}$ which are shown in Fig. 3. The second derivatives, changed of sign, of these functions are displayed and compared with the experimental spectrum in Fig. 4.

Although the experimental ELS result is much smoother, due to the obviously lower resolution, there is a clear correspondence between calculated surface and bulk contributions and measured spectra up to 10 eV. At 10 eV optical data have a peak which is missing in the experiment. At higher energy the measured spectrum is somewhat intermediate between the bulk and the surface curves.

Since the two are never very different from one another, it is clearly problematic to distinguish between bulk and surface losses in Fe. This is also shown by the lack of any strong E_p dependence of Fig. 1.

The ELS spectrum is generally very rich in structures. What is the significance to be attached if any, to peaks and minima of $M(E)$?

The answer to this question is provided directly by Fig. 5, where the bulk loss function, its second derivative, changed of sign, and the optical conductivity (all constructed from optical data) are compared. The peaks of $(-d^2/dE^2)[-\mathrm{Im}(\tilde{\epsilon})^{-}]$ correspond well with the peaks of $-\mathrm{Im}(\tilde{\epsilon})^{-1}$ itself. Each such peak indicates a damped longitudinal excitation in the system, that is, by Maxwell's equation $i\vec{q}\cdot\vec{E}=4\pi\rho^{\mathrm{tot}}$, one where the electron charge density also oscillates. Often these oscillations are named "collective" to emphasize the effect that bodily motion of all electrons is necessary to generate the macroscopic field $\vec{E}$.

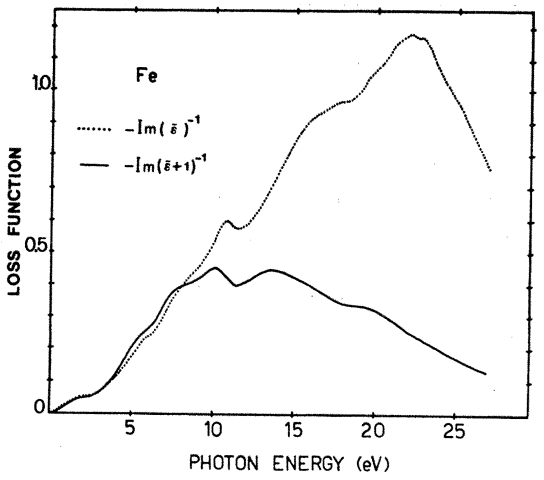

FIG. 3. Bulk and surface loss functions calculated from the optical data (Ref. 3), via Kramers-Kronig analysis.

In a metal it is also customary to name "plasmon" the strongest collective excitation—though clearly this concept may become ill defined in some cases. Clearly with this definition the plasmon in Fe is expected from optical data around 22 eV as the main peak of $N(E)$. Figures 3 and 5 do in fact show clearly that the plasmon is the main high-energy feature of the optical $N(E)$ and locate it at 22.4 ± 0.5 eV. The other peak of $N(E)$, instead, corresponds to minor longitudinal excitations, that occur in connection with—but not at the same energy as—band-to-band transitions.

A second message contained in Fig. 5, which is not universaly acknowledged is that *minima* of $N(E)$ [that are peaks of $-M(E)$] are in excellent correspondence with optical absorption peaks. Therefore, strong interband transitions can be immediately traced on an ELS spectrum, by looking at the minima, rather than at the maxima, as is sometimes done.

This connection between interband transitions and minima in ELS spectra can also be shown to follow from the algebraic connection between $\sigma(E)$ and $-M(E)$ by means of simple models.[11] Figure 6 shows a direct comparison of the experimental $-M(E)$ with $\sigma(E)$. The agreement is fairly good—as indicated by the dashed lines—for all peaks except for one at 10 eV, which is totally absent in optics. This finding will be discussed in Sec. V.

IV. BAND-STRUCTURE AND SINGLE-PARTICLE EXCITATIONS

Several experimental methods have been used to test the band-structure calculations of Fe. de Haas–van Alphen studies have been used to map the Fermi surface and extensive optical works[2,3] have provided information on the location of the bands several eV above and below the Fermi level. Angle-resolved photoemission measurements[5] have determined band dispersion along the Γ-P-H direction in the Brillouin zone.

Our ELS spectra extend beyond the energy region tested so far and we can give therefore valuable information on the high-lying conduction bands which have often been proven to be rather

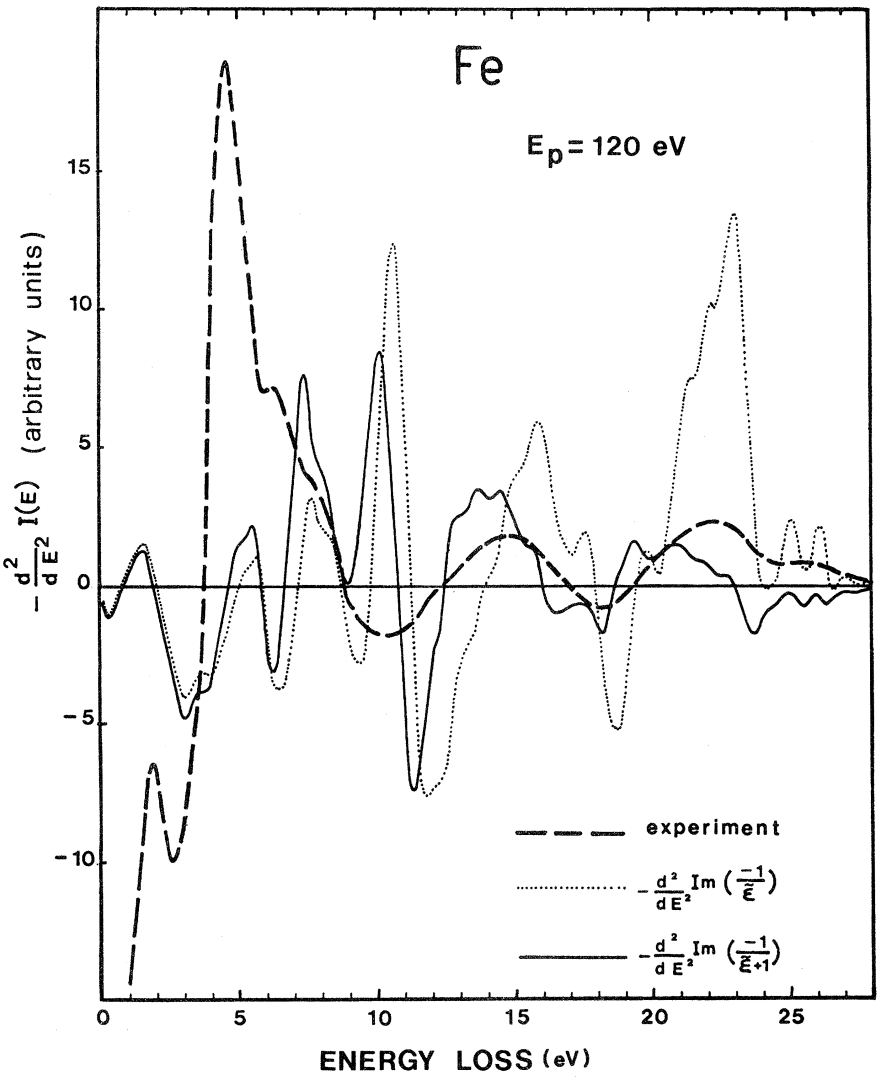

FIG. 4. Comparison of ELS measurements ($E_p = 120$ eV) and the second derivative, changed of sign, of bulk and surface loss functions obtained from optical data (Ref. 3).

critical. Figure 7 shows recent spin-split energy bands as calculated by Callaway and Wang[19] and in Fig. 8 we report the energy position along high-symmetry lines or at symmetry points where single-particle excitations can be expected on the basis of this band-structure calculation. Since electron excitations can induce multipole transitions, both dipole and multipole transitions are reported. The first line in Fig. 8 reports the energies for which single-particle excitations are found in our ELS spectra. The first one of these energies is 2.5 eV. This excitation is in good agreement with the optical transition found by Weaver *et al.*[2] at 2.37 eV. In agreement with Weaver *et al.* we interpret it as a transition between nearly flat bands along the Σ and D directions. The next structure occurs at 5.9 eV and is the counterpart of the optical transition found by Moravec *et al.*[3] at 6.1 eV. The attribution of this transition is not easy since it does not correspond to any of the theoretical transitions of Fig. 8. The closest theoretical transition occurs along F and is displaced to higher energies by 1 eV.

The structure around 10 eV is a superposition of a dipole-allowed transition at 9.1 and 12 eV (observed also in optical experiment) and a multipole transition at 10.4 eV (which is not seen in optical spectra). This last excitation can be associated with transitions at N. Its origin and interpretation will be discussed in more detail in the following

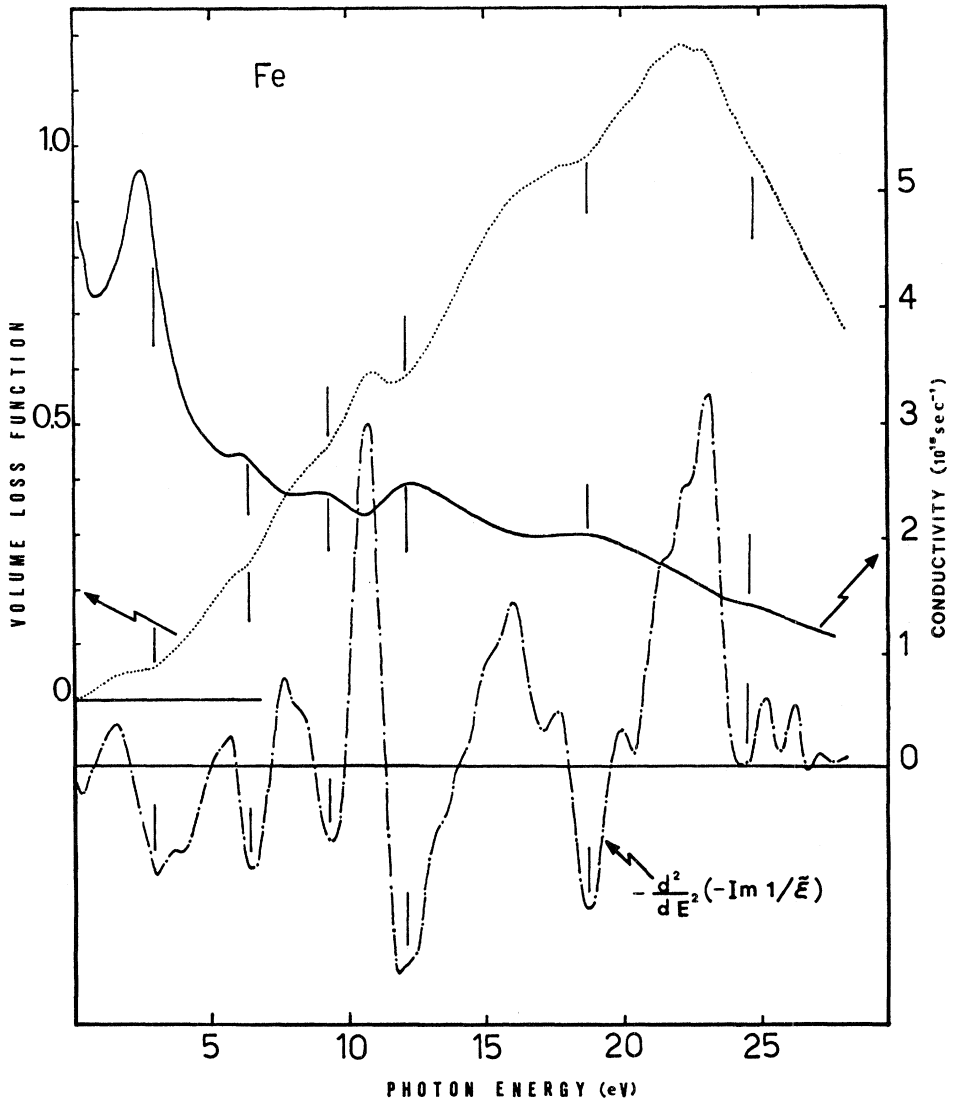

FIG. 5. Dotted line: volume loss function of Fe as calculated from optical studies. Solid line: optical conductivity. Dashed-dotted line: second derivative, changed of sign, of volume loss function.

section.

The excitations at 9.1 and 12 eV originate probably along F although the theoretical energies of these transitions are again about 1 eV larger than the experimental ones. The next excitation occurs at about 18.4 eV in our ELS spectra. This should correspond to the optical feature at 19 eV and Fig. 8 shows that it should be associated to transitions at N. Its attribution is uncertain at present since it would require extending the calculation to higher energies. The last ELS excitation occurs at about 25 eV. It could be associated to optical transition at N and to multipole transitions at H, which, however, should be much more observable as will be discussed in the following section.

V. SELECTION RULES: QUADRUPOLE VERSUS DIPOLE TRANSITIONS

In this section we discuss the selection rules to be used when trying to connect the ELS spectrum to the one-electron band structure. The present discussion will concentrate on bulk losses only, as relevant to the interpretation of our results in Fe. Selection rules in ELS spectra, also applied to sur-

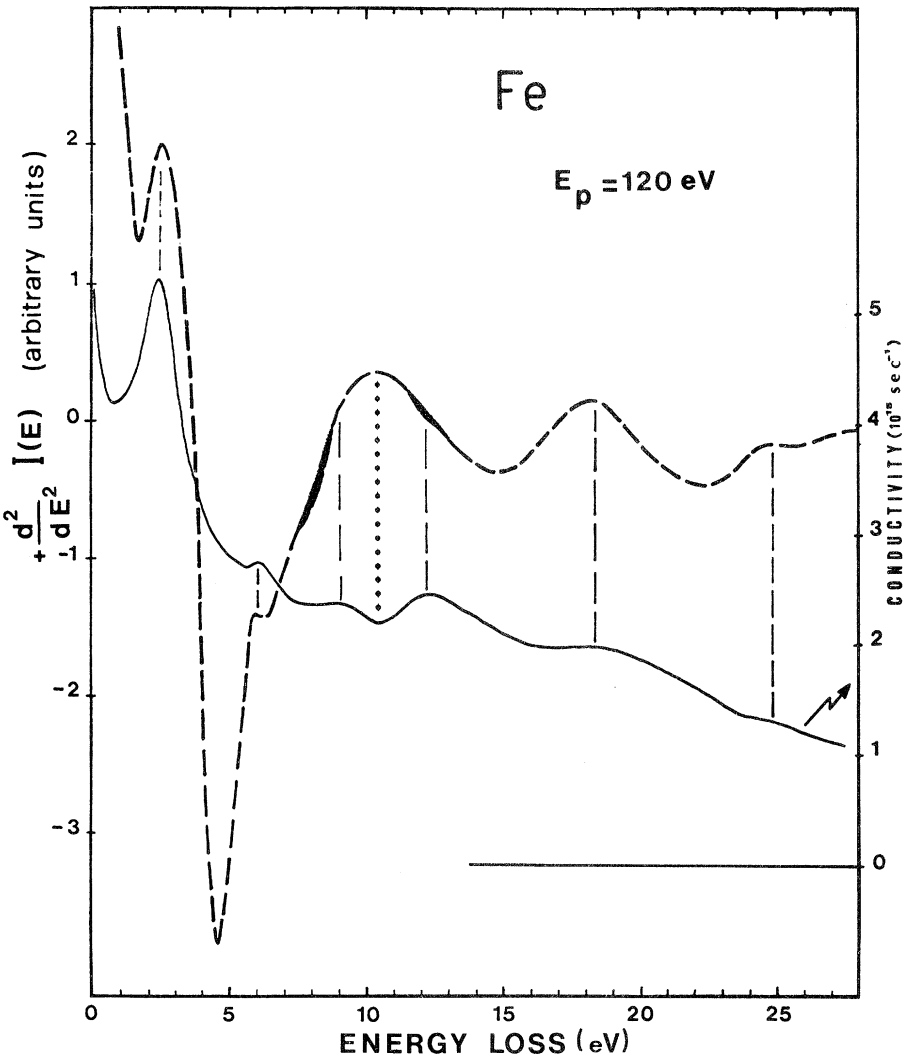

FIG. 6. Comparison of the optical conductivity and the experimental ELS spectrum changed of sign. The peaks of the curves indicate the energy positions of optical interband transitions in Fe. The dotted line points out the exception to the one-to-one correspondence among maxima of optical and ELS measurements. The shaded areas represent the surface contributions in our ELS spectra. They do not have a counterpart in the optical conductivity.

face losses, have been discussed previously, among others, by Ludeke and Koma[12] and by Rubloff.[20]

Qualitatively, there are two kinds of processes by which the loss process against the electrons of the system can occur. One is direct Coulomb scattering: The primary electron $(E_p, \vec{k}_p)$ loses some energy and momentum $(E, \vec{q})$ by collision with one system electron, and is then detected in the state $(E_p - E, \vec{k}_p - \vec{q})$. The other is exchange scattering, where the primary electron $(E_p, \vec{k}_p)$ kicks off another electron, which is detected in the state $(E_p - E, \vec{k}_p - \vec{q})$ and falls down to take its place. The latter process is expected to be of importance only when the primary electron energy E_p is low enough, e.g., comparable to E_F. It can lead, for example, to a small reduction in the cross section for plasmon creation near threshold,[21] and also to inelastic spin-flip scattering,[22] a process whose cross section in direct scattering is zero in the absence of spin-orbit coupling. We shall restrict our attention here to direct processes, as our lowest primary energy, 50 eV, is already one order of magnitude above the typical valence energies in Fe.

The primary electron acts upon the one-electron states in the crystal as any charged (longitudinal) external probe, characterized by a space and time-

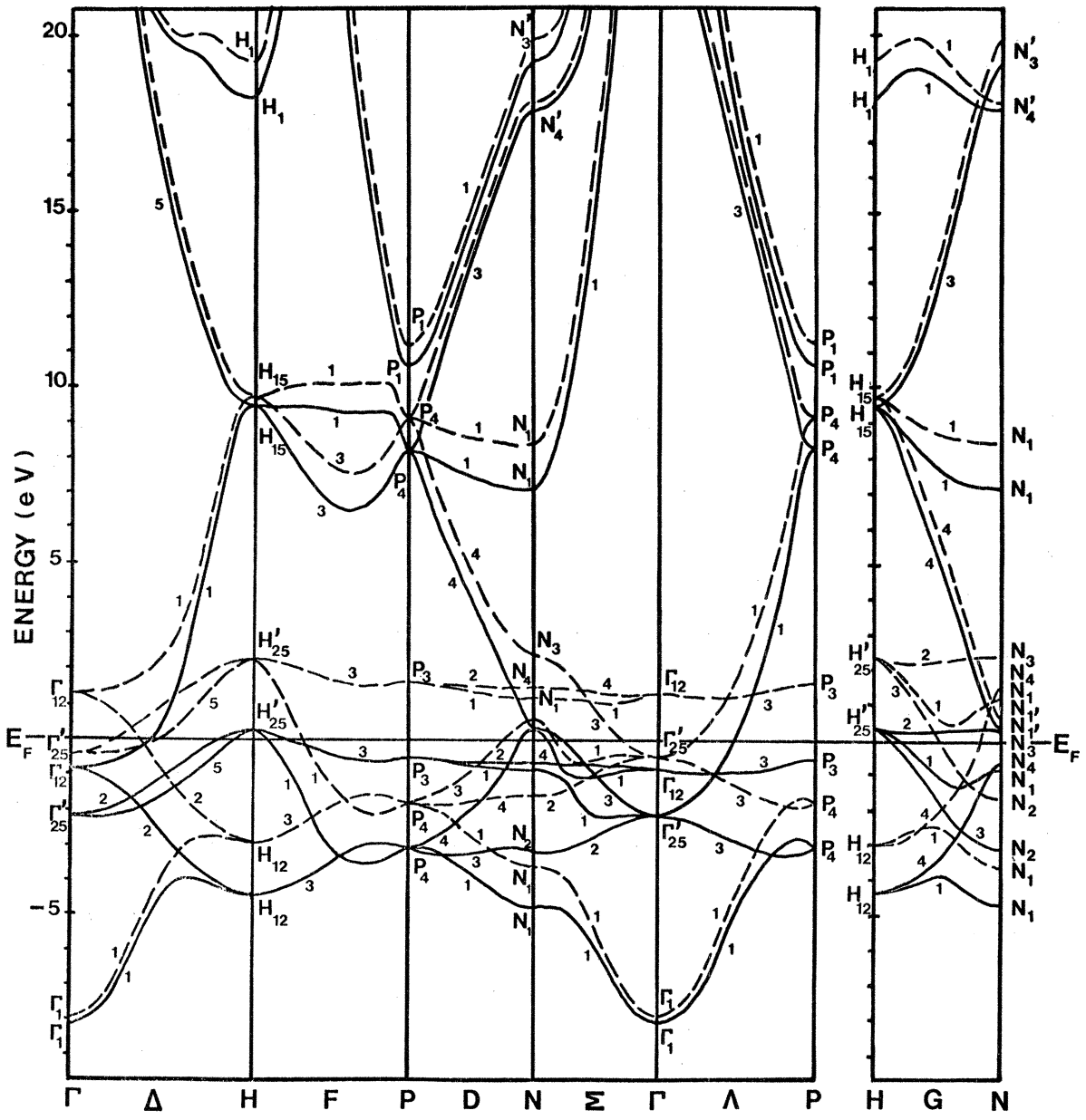

FIG. 7. Energy-band structure of ferromagnetic Fe as calculated by Callaway and Wang (Ref. 6) and private communication (Callaway). Solid line: majority-spin energy levels. Dashed line: minority-spin energy levels.

varying density $\rho(\vec{r},t)$, via the perturbing Hamiltonian

$$H'(r,t)=\sum_{\vec{q}E}\rho_{qE}\frac{4\pi e^2}{q^2}\exp[-i(\vec{q}\cdot\vec{r}-\omega t)]\ , \quad (5.1)$$

where ρ_{qE} is the Fourier transform of $\rho(\vec{r},t)$, and depends on the electronic trajectory. Interband transitions $|k,l\rangle\rightarrow|k+q,l'\rangle$ can occur due to H', provided energy and momentum can be conserved, and provided the matrix element

$$T=\langle k,l\,|\exp(-i\vec{q}\cdot\vec{r})\,|k+q,l'\rangle \quad (5.2)$$

does not vanish.

The selection rules required by symmetry for T are obtained, as usual[23] by expanding T in powers of q or, as it turns out, in powers of $(\vec{q}\cdot\vec{r})$: a multipole expansion.[24] We write

$$T=M+D+Q+\cdots\ , \quad (5.3)$$

where M is q independent, D is linear in $(\vec{q}\cdot\vec{r})$, Q quadratic, in $(\vec{q}\cdot\vec{r})$, etc. The typical magnitude of

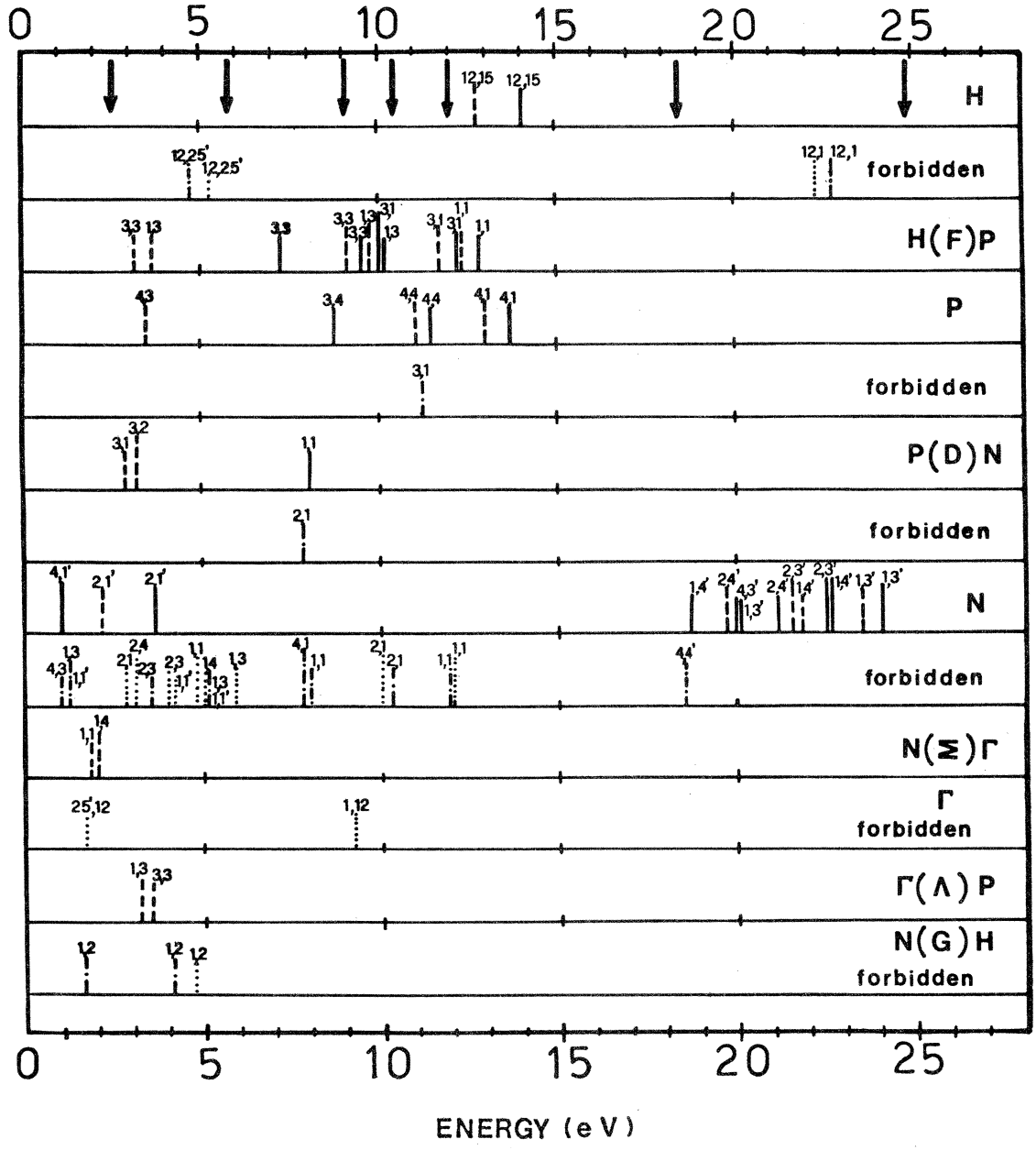

FIG. 8. Energy position of expected single-particle contributions in ELS spectra of Fe as obtained from Fig. 7. Solid line: spin-up—spin-up transitions, dashed lines: spin-down—spin-down transitions, dashed-dotted lines: spin-up—spin-up dipole-forbidden transitions, dotted lines: spin-down—spin-down dipole-forbidden transitions. The arrows in the top line show our experimental determinations.

a matrix element of $(\vec{q}\cdot\vec{r})$ can be estimated as follows. The loss rate for energy $\hbar\omega$ is largest for $q<\omega/v_p$, where $v_p=\sqrt{2E_p/m}$ is the incident electron's velocity in vacuum. On the other hand, the typical length scale for the spatial variation of a Bloch function $|k,l\rangle$ is the lattice parameter a. Hence, we expect that successive powers of $(\vec{q}\cdot\vec{r})$ will scale roughly by the factor

$$f_{\rm el}=\frac{\omega}{v_p}a \tag{5.4}$$

It is instructive to contrast this situation with the alternative case of optics. There, the external perturbation is

$$H'_{\rm opt}=\frac{e}{mc}\vec{A}\cdot\vec{p}\exp[-i(\vec{k}_0\cdot\vec{r}-\omega t)]+\text{ c.c.} \tag{5.5}$$

where $\vec{A}$ is the vector potential, and $k_0 = n(\omega/c)$ if $\hbar\omega$ is the photon energy and n the refractive index. In optics, successive powers of $(\vec{k}_0 \cdot \vec{r})$ differ roughly by a factor

$$f_{\text{opt}} = \frac{\omega}{c/n} a \ . \tag{5.6}$$

Clearly, under ordinary conditions, $f_{\text{opt}} << f_{\text{el}}$. For example, for $\hbar\omega = 10$ eV $f_{\text{opt}} \simeq 10^{-2}$, while at $E_p = 100$ eV, f_{el} is still of order 1. In conclusion, higher multipole transitions, rarely of noticeable strength in optics,[23] must as a rule be well observable with electrons, especially if they are slow, and they lose a large fraction of their energy. This fact is well known and has been exploited by many workers, e.g., by Ludeke and Koma,[12] and by Ritsko, Brillson, and Sandmans,[25] to quote only a few.

Here, we shall first consider quite generally each term of the multipole expansion (5.3) up to the quadrupole. Subsequently, the quadrupole transitions will be considered for the special case of Fe. The monopole interband term is of course zero, $M = \langle k,l \mid k,l' \rangle = 0$, because of the orthogonality of Bloch functions.

The dipole term is obtained as

$$D = -i\vec{q}\langle k,l \mid \vec{r} - i\hbar\vec{p}/m(E_{kl} - E_{kl'}) \mid k,l' \rangle \tag{5.7}$$

where the first piece comes from expanding the phase factor $\exp(-i\vec{q}\cdot\vec{r})$, and the second from a $(\vec{q}\cdot\vec{p}\,)$ expansion of $\mid k+q,l' \rangle$. Inversion symmetry has been used in the derivation of the last piece, in the form $\langle k,l' \mid \vec{p} \mid k,l' \rangle = 0$. The two pieces in (5.7) are actually equal, by virtue of the well-known relationship between matrix elements of $\vec{r}$ and of $\vec{p}$ for single-particle eigenstates.[26] The dipole selection rules for D, obtained by group theory, are well known from optics. They are given explicitly for all relevant points and lines in the bcc Brillouin zone by Eberhardt and Himpsel,[27] and will not be reproduced here.

The quadrupole term is obtained in the form

$$Q = -\left\langle k,l \left| \left[\tfrac{3}{2}(\vec{q}\cdot\vec{r})^2 + \sum_{l''} \frac{E_{kl''} - E_{kl}}{E_{kl'} - E_{kl}} (\vec{q}\cdot\vec{r}) \mid k,l'' \rangle\langle k,l'' \mid (\vec{q}\cdot\vec{r}) \right] \right| k,l' \right\rangle \ . \tag{5.8}$$

We note that the two pieces inside square brackets have the same symmetry, i.e., they link all and the same states $\langle k,l \mid$ and $\mid k,l' \rangle$. This is seen, e.g., by means of the identity

$$(\vec{q}\cdot\vec{r})^2 = \sum_{l''} (\vec{q}\cdot\vec{r}) \mid k,l'' \rangle\langle k,l'' \mid (\vec{q}\cdot\vec{r}) \tag{5.9}$$

which shows that the first piece and the second have the same structure, except for the numerical factor $(E_{k,l''} - E_{k,l'})/(E_{k,l'} - E_{kl})$. For either of them to be nonzero at least one intermediate state $\mid k,l'' \rangle$ must exist for which

$$\langle k,l \mid (\vec{q}\cdot\vec{r}) \mid k,l'' \rangle\langle k,l'' \mid (\vec{q}\cdot\vec{r}) \mid k,l' \rangle$$

is nonzero. If such a state exists to make $\langle k,l \mid (\vec{q}\cdot\vec{r})^2 \mid k,l' \rangle$ nonzero, the second piece also will in general yield a finite contribution, since a symmetry-based selection rule cannot depend on the actual energies E_{kl} involved in the numerical factor.

We have derived the quadrupole selection rules for interband transitions at all important k points in the Brillouin zone of a bcc crystal. The direction of $\vec{q}$ relative to the crystal axes is assumed to be random. With this assumption, our results are directly applicable to the ELS spectra of either a single crystal with general orientation, or as is the case in the present experiment, of a polycrystalline sample. Stricter selection rules would apply for $\vec{q}$ along a crystalline axis.

The resulting quadrupole-allowed (but dipole-forbidden) interband transitions in Fe, as described in the ferromagnetic state by the band structure of Callaway and Wang,[19] are shown in Table I. As shown by comparison with Fig. 8, a vast majority of dipole-forbidden transitions have become quadrupole allowed, and should show up in the ELS spectra. There they ought to be most evident for low E_p, and large $\hbar\omega$.

It is clear from, e.g., Figs. 1, 2, and 4, that the ELS resolution is not good enough to allow detection of these transitions one by one. However, it can allow the detection of groups of transitions. We can identify in Table I three broad groups of transitions. The first group consists of many transitions around and below 5 eV. These are transitions within the d band itself. A second group of transitions is centred around 10 eV, and a third, consisting of two transitions only, around 22 eV. These latter two groups correspond to transitions

TABLE I. Quadrupole-allowed interband transitions in ferromagnetic Fe. The notation of Callaway and Wang (Ref. 6) is adapted throughout.

k point and interband energy (eV)	Γ	$\hbar\omega$	H	$\hbar\omega$	P	$\hbar\omega$	N	$\hbar\omega$	D	$\hbar\omega$	G	$\hbar\omega$
Group	O_h		O_h		T_d		D_{2h}		C_{2v}		C_{2v}	
$(\vec{q}\cdot\vec{r})^2$	$12+25'$		$12+25'$		$3+4$		$1+2+3+4$		$1+2+3+4$		$1+2+3+4$	
Quadrupole-allowed transitions	$25'\downarrow\rightarrow 12\downarrow$	1.8					$4\uparrow\rightarrow 3\uparrow$	1.0				
							$1\uparrow\rightarrow 3\uparrow$	1.2			$1\uparrow\rightarrow 2\uparrow$	1.6
							$2\downarrow\rightarrow 1\downarrow$	2.7				
							$2\downarrow\rightarrow 4\downarrow$	3.0				
							$2\uparrow\rightarrow 3\uparrow$	3.2				
			$12\uparrow\rightarrow 25'\uparrow$	4.5			$2\downarrow\rightarrow 3\downarrow$	3.6			$1\uparrow\rightarrow 2\uparrow$	4.0
							$1\downarrow\rightarrow 1\downarrow$	4.6			$1\downarrow\rightarrow 2\downarrow$	4.7
							$1\downarrow\rightarrow 4\downarrow$	4.9				
			$12\downarrow\rightarrow 25'\downarrow$	5.0			$1\uparrow\rightarrow 3\uparrow$	5.0				
							$1\downarrow\rightarrow 3\downarrow$	5.8				
							$4\uparrow\rightarrow 1\uparrow$	7.6				
	$1\downarrow\rightarrow 2\downarrow$	9.0					$3\uparrow\rightarrow 1\uparrow$	8.0	$2\uparrow\rightarrow 1\uparrow$	8.0		
							$2\downarrow\rightarrow 1\downarrow$	10.0				
							$2\uparrow\rightarrow 1\uparrow$	10.3				
							$1\uparrow\rightarrow 1\uparrow$	11.8				
					$3\uparrow\rightarrow 1\uparrow$	11.5	$1\downarrow\rightarrow 1\downarrow$	12.0				
			$12\downarrow\rightarrow 1\downarrow$	22.0								
			$12\uparrow\rightarrow 1\uparrow$	22.5								

from the filled d states to vastly plane-wave-like final states that should have a large s admixture.

In order to detect possible evidence for quadrupole-allowed transitions, we consider in the first place the direct comparison of the ELS spectrum with the frequency-dependent conductivity obtained by optics (Fig. 6). The sign of the ELS spectrum is reversed, so that now peaks should correspond to interband transitions; that is to peaks of optical conductivity. Since the latter obeys dipole selection rules, any quadrupole transitions should show up as a peak in ELS, which is missing in optics.

Figure 6 shows that the correspondence between ELS and optics is, in general, excellent, with a one-to-one correspondence of transitions. There is, however, one macroscopic exception, a broad ELS peak around 10 eV which has no optical counterpart. This feature is thus tentatively ascribed to the second group of quadrupole transitions described above, centered about the saddle point $N_{2\uparrow\downarrow}\rightarrow N_{1\uparrow\downarrow}$ and $N_{1\downarrow\uparrow}\rightarrow N_{1\downarrow\uparrow}$. No such unique feature is found at and below 5 eV or above 20 eV, where peaks exist both in the ELS spectrum *and* in the optical conductivity. The absence of any new isolated structure at low energy may be interpreted as due to the very high density of quadrupole-allowed transitions, and also to the fact that $f_{\rm el}$ may be too small in this regime. As for the high-energy transitions, we observe that first of all the peak around 25 eV is in fact stronger in ELS than in optics. Secondly, its intensity grows very strongly for decreasing electron energy, as shown by Fig. 1 (beware of the sign reversal between Figs. 6 and 1). Hence, it seems likely that the second group of two quadrupole-allowed transitions, predicted by theory to be centered about $H_{12\uparrow\downarrow}\rightarrow H_{1\uparrow\downarrow}$ at 22 eV, can actually be identified with a broad ELS structure centered at 24.8 eV.

VI. OXYGEN CONTAMINATION AND SURFACE EFFECTS

ELS spectra taken in the reflection mode are known to show, as we have already pointed out, both bulk and surface excitations.[28,29] We note very few characteristic surface features in our ELS spectra and the similarity between the volume and the surface-loss functions (Fig. 4) makes it difficult to separate the two contributions. The dependence on surface contamination and on primary electron energies helps to distinguish among bulk and surface excitations. We have shown that peaks A, B, F, G, and H do not exhibit a strong dependence on the surface oxygen contamination (Fig. 2). They

TABLE II. Surface and bulk (longitudinal) excitations and single-particle (transverse) excitations in Fe.

	A	*B*	*C*	*D*	*E*	*F*	*G*	*H*
Volume	1.9	4.6	6.3			14.7	22.4	26.7
Collective (longitudinal) excitations								
Surface				8.3[a]	12.0			
Single-particle interband (transverse) excitations	2.5	5.9	7.5[a]	9.1[b] 10.4	12.1[b]	18.4	24.8	

[a]These features could be due to a very small amount of residual oxygen ($\lesssim$0.02 monolayer).
[b]These values have been taken from Ref. 3.

are interpreted, therefore, as bulk excitations. Peak *E* is more pronounced in the low E_p spectra and this suggests that it is due to a surface excitation. This interpretation is confirmed by the spectra taken as a function of oxygen coverage.

The nature of peak *D* is somewhat less clear. Even though the average coverage of oxygen on our "clean" Fe surfaces is below 0.02 monolayers during ELS run, we suspect that peak *D* is oxygen induced. This interpretation is suggested by the coincidence of peak *D* with the strong oxygen-induced features at 8 eV. It could be related to oxygen levels which form bound states at about 8 eV below Fe Fermi level in the iron oxides. An alternative interpretation of the shoulder *D* as a genuine Fe feature in our clean spectra cannot be ruled out at the moment.

Peak *C* is more intense in the high E_p spectra and therefore it seems to be due to a bulk loss. Its dependence on oxygen coverage is probably only apparent due to the rapid growth of the oxygen induced loss at 8 eV. In Table II we summarize our results on bulk and surface excitations in ferromagnetic iron. The results inferred from ultraviolet optical data[3] are also shown.

VII. CONCLUSIONS

The main results of this work can be summarized as follows:

(a) The amount of spectroscopic information obtained by ELS is not less detailed than that of optics. As can be anticipated on general grounds and as verified in the case of Fe, all absorption peaks correspond extremely well to *minima* of $(-d^2/dE^2)$ $[EN(E)]$, rather than to maxima as it is sometimes assumed.

(b) Interband transitions of Fe up to 25 eV are identified by comparison with the band-structure calculation up to high energies of Callaway and Wang. On the whole this band structure is found to be accurate, including several high-energy-empty states.

(c) The problem of higher multipole transitions is considered, and quadrupole selection rules as applicable to bcc Fe are worked out. One remarkable new absorption structure around 10 eV which is found in ELS but is absent in optics is assigned to a group of quadrupole-allowed transitions in the Callaway and Wang band structure.

(d) While the main bulk collective excitation, that may be called the bulk plasmon, is clearly seen at 22.4 eV, its surface-plasmon counterpart is not seen as distinctly in the ELS spectrum of Fe. Also the amount of other surface-related features are tested by means of oxygen contamination, and found to be generally small. What is found, instead, is a new oxygen-related absorption peak at $\sim$8 eV.

ACKNOWLEDGMENTS

We are indebted to P. Perfetti, S. Nannarone, and S. Modesti for helpful discussions and technical suggestions. We thank Professor J. Callaway for providing us a computer list of Fe band calculations. We have greatly appreciated the critical comments on the manuscript by G. Margaritondo. Also the continuous and invaluable technical help of T. Mazzei is gratefully acknowledged.

[1]M. B. Stearns, Phys. Rev. B 8, 4383 (1973); 13, 1183 (1976).

[2]A large amount of references on optical and photoemission works on Fe can be found in J. H. Weaver, E. Colavita, D. W. Lynch, and R. Rosei, Phys. Rev. B 19, 3850 (1979).

[3]T. J. Moravec, J. C. Rife, and R. N. Dexter, Phys. Rev. B 13, 3297 (1979).

[4]P. Heimann, E. Marschall, H. Neddermayer, M. Pessa, and H. Roloff, Phys. Rev. B 16, 2575 (1977); P. Heimann and H. Neddermayer, Phys. Rev. B 18, 3537 (1978).

[5]D. E. Eastman, F. J. Himpsel, and J. A. Knapp, Phys. Rev. Lett. 44, 95 (1980).

[6]J. Callaway and C. S. Wang, Phys. Rev. B 16, 2095 (1977).

[7]H. Froitzheim, in *Electron Energy Loss Spectroscopy,* Vol. 4 of *Electron Spectroscopy for Surface Analysis—Topics in Current Physics* edited by H. Ibach (Springer, New York, 1977).

[8]H. Raether, in *Excitation of Plasmon and Interband Transitions by Electrons,* Vol. 88 of *Springer Tracts in Modern Physics,* edited by H. Ralther (Springer, New York, 1980).

[9]W. K. Schubert and E. L. Wolf, Phys. Rev. B 20, 1855 (1980).

[10]L. Papagno, E. Colavita, L. S. Caputi, G. Chiarello, M. De Crescenzi, R. Scarmozzino, and R. Rosei (unpublished).

[11]L. S. Caputi, E. Colavita, M. De Crescenzi, S. Modesti, L. Papagno, R. Scarmozzino, R. Rosei, and E. Tosatti, Solid State Commun. 39, 117 (1981).

[12]R. Ludeke and A. Koma, Phys. Rev. Lett. 34, 817 (1975).

[13]R. H. Ritchie, Phys. Rev. 106, 874 (1957).

[14]A. A. Lucas and M. Sunjic, in *Fast-electron Spectroscopy of Collective Excitations in Solids* in Vol. 2 part 2 of *Progress in Surface Science* edited by S. G. Davison (Pergamon, New York, 1972).

[15]See, e.g., I. Lindau and W. E. Spicer, J. Electron Spectrosc. Relat. Phenom. 3, 409 (1974).

[16]G. Chiarello, L. S. Caputi, E. Colavita, M. De Crescenzi, L. Papagno, R. Scarmozzino, and R. Rosei (unpublished).

[17]V. E. Henrich, G. Dresselhaus, and H. Zeiger, Phys. Rev. B 22, 4764 (1980).

[18]Of course, the optical $\tilde{\epsilon}(E)$ is transverse, and in principle different from the longitudinal $\tilde{\epsilon}(E)$ seen in ELS. However, both probes are sufficiently close when $q=0$, so differences between the two ought to be small, *except* for forbidden transitions as discussed in Sec. V.

[19]J. Callaway and C. S. Wang, Phys. Rev. B 16, 2095 (1977), and private communication. We wish to thank Professor Callaway for providing us with unpublished results on the high-energy region of the band structure of Fig. 7.

[20]G. W. Rubloff, Solid State Commun. 26, 523 (1978).

[21]Soe Yin, B. Goodman, and E. Tosatti (unpublished).

[22]Soe Yin and E. Tosatti (unpublished).

[23]See, e.g., H. A. Bethe and E. E. Salpeter, *Quantum Mechanics of One- and Two-electron Systems* (Springer, Berlin, 1957).

[24]J. D. Jackson, *Classical Electrodynamics* (Wiley, New York, 1962).

[25]J. J. Ritsko, L. J. Brillson, and D. J. Sandman, Solid State Commun. 24, 109 (1977).

[26]See, e.g., L. I. Schiff, *Quantum Mechanics* (McGraw-Hill, New York, 1968), Chap. 44.

[27]W. Eberhardt and F. J. Himpsel, Phys. Rev. B 21, 5572 (1980).

[28]Y. Ballu, J. Lecante, and H. Rousseau, Phys. Rev. B 14, 3201 (1976).

[29]L. Braicovich, G. Rossi, R. A. Powell, and W. E. Spicer, Phys. Rev. B 21, 3539 (1980).